

Florida State University Libraries

2016

Adjustment of Visually Observed Ship Winds (Beaufort Winds) in ICOADS

Keqiao Li



FLORIDA STATE UNIVERSITY
COLLEGE OF ARTS AND SCIENCES

ADJUSTMENT OF VISUALLY OBSERVED SHIP WINDS (BEAUFORT WINDS)

IN ICOADS

By

KEQIAO LI

A Thesis submitted to the
Department of Earth Oceanic and Atmospheric Science
in partial fulfillment of the
requirements for the degree of
Master of Science

2016

Keqiao Li defended this thesis on March 29, 2016.

The members of the supervisory committee were:

Mark A. Bourassa
Professor Directing Thesis

Shawn R. Smith
Committee Member

Guosheng Liu
Committee Member

Jeffrey Chagnon
Committee Member

The Graduate School has verified and approved the above-named committee members, and certifies that the thesis has been approved in accordance with university requirements.

ACKNOWLEDGMENTS

This work has been supported by the Climate Observation Division, Climate Program Office, National Oceanic and Atmospheric Administration, U.S. Department of Commerce, ('under grant NA11OAR4310169) for the ICOADS Value Added Dataset development and the NASA Physical Oceanography for the NASA Ocean Vector Winds Science Team.

Firstly, I would like to express my sincere gratitude to my major professor, Dr. Mark A. Bourassa, for the continuous support of my studies and research, and for his patience, motivation, and immense knowledge. His guidance helped me throughout my research and in the writing of this thesis.

In addition to my major professor, I would like to thank Mr. Shawn R. Smith. I appreciate his guidance and patience throughout these two years of graduate studies.

I would also like to thank the other members of my committee, Drs. Guosheng Liu and Jeffrey Chagnon, for their insightful comments and encouragement.

Special thanks go to Tracy Ippolito, writing coach at Center for Ocean-Atmospheric Prediction Studies (COAPS), for her assistance in preparing the thesis manuscript. In addition, I would like to give a big thanks to Jocelyn Elya, lead programmer at COAPS, for her invaluable help with the programming aspects of my research.

I would also like to express my deep gratitude to all of the graduate students and research scientists at COAPS who have provided helpful suggestions.

Last, but not least, I wish to thank my family for their constant love and support that helps make it possible for me to endure all difficulties and makes me stronger.

TABLE OF CONTENTS

List of Tables	v
List of Figures	vi
Abstract	viii
1. INTRODUCTION	1
2. DATA	4
2.1. ICOADS visually estimated ship wind speed dataset	4
2.2. Scatterometer wind speed dataset	11
2.3. Equivalent neutral wind	12
2.4. Quality control	13
3. METHODOLOGIES	15
3.1. Collocation between satellite scatterometer winds and visually estimated ship winds	15
3.2. Modification of the calibration due to statistical artifacts	16
3.3. Assessment of system errors as a function of wind speed	17
3.4. Significance test	19
4. RESULTS AND DISCUSSION	20
5. CONCLUSION	29
References	31
Biographical Sketch	35

LIST OF TABLES

Table 1. Applying the Lindau's (1995) scale. Lindau (1995) values are converted to ms^{-1} by multiplying by 0.5144 and rounding to one decimal place. Deck 761 contained no wind speeds associated with Beaufort force 12	7
Table 2. Statistical significance test for deck 792 and deck 992. Those P-values less than α are bolded.....	26
Table 3. Bias correction for decks 792 and 992.....	27
Table 4. The comparison between Lindau's (1995) correction and LMS	28

LIST OF FIGURES

Figure 1. Histogram of wind speed with WI= 5	6
Figure 2. Histogram of wind speed with WI=5 with deck 761. Each peak's count is labeled	6
Figure 3. Histogram of Wind speed with (a) WI=0 (Meter per second, estimated); (b) WI=3 (Knot, estimated); (c) WI=6 (Estimated (original units unknown or unknown method)).	8
Figure 4. Histogram of wind speed with WI=0 categorized by major decks (a) Deck 732:Russian Marine Met. Data Set (MORMET) (rec'd at NCAR). (b) Deck 792:US National Centers for Environmental Prediction (NCEP) BUFR GTS: Ship Data. (c) Deck 888: US Air Force Global Weather Central (GWC). (d) Deck 892:US National Centers for Environmental Prediction (NCEP) Ship Data. (e) Deck 926: International Maritime Meteorological (IMM) Data.....	9
Figure 5. Histogram of wind speed with WI=3 categorized by major decks. (a) Deck 254: UK Met. Office (MetO) Main Marine Data Bank (MDB). (b) Deck 667:Inter-American Tropical Tuna Commission (IATTC) (c) Deck 792: US National Centers for Environmental Prediction (NCEP) BUFR GTS: Ship Data. (d) Deck 892: US Natl. Centers for Environmental Pred. (NCEP) Ship Data. (e) Deck 926: International Maritime Meteorological (IMM) Data. (f) Deck 927: International Marine (US-or foreign-keyed ship data, 1970-2007)	10
Figure 6. Histogram of wind speed with WI=6 categorized by major decks. (a) Deck 128: International Marine (US-or foreign-keyed ship data, 1950-1978). (b) Deck 555: US Navy Fleet Numerical Meteorology and Oceanography Center (FNMOC; Monterey) Telecom. (c) Deck 888: US Air Force Global Weather Central (GWC). (d) Deck 892: US National Centers for Environmental Prediction (NCEP) Ship Data. (e) Deck 927: International Marine (US-or foreign-keyed ship data, 1970-2007)	11
Figure 7. Map for collocated estimated ship winds. Red dots are associated with location of collocated estimated ship winds. The limited spatial sample is related to the satellite coverage at the times of day of the ship observations.....	16
Figure 8. The density plot for the collocation wind speed scatter plot categorized by major decks for the period Nov. 1999-Oct. 2009. The contour line is density contours, which are associated with the number of data points fell into a $1\text{ms}^{-1} \times 1\text{ms}^{-1}$ box. The green line is reference line. The red line is simple linear fit line. (a) The density plot for deck 792; (b) The density plot for deck 926; (c) The density plot for deck 992	21
Figure 9. The boxplots for three different major deck (792, 926, and 992). Each one of the whisker box is associated with the number of data points in a range of 2ms^{-1} of scatterometer wind speed. The width of each whisker box is proportional to the data points within each 2ms^{-1} bin. (a) Deck 792; (b) Deck 926; (c) Deck 992	22

Figure 10. Same as Figure 9. The black dots are associated with conditional sample mean of each 0.5m/s bin of the simulated error-free dataset. (a) Deck 792; (b) Deck 926; (c) Deck 992).....24

Figure 11. Same as Figure 9. The black dots are associated with conditional sample mean of each 0.5ms⁻¹ bin of simulated scatterometer winds generated by Monte Carlo approach. Red line is the cubic fitting line for those black dots (conditional sample mean). (a) Deck 792; (b) Deck 926; (c) Deck 992.....25

ABSTRACT

The bias adjustment of visually estimated ship winds in the International Comprehensive Ocean-Atmosphere Data Set (ICOADS) is addressed through the comparison to the QuickSCAT scatterometer equivalent neutral winds. We assume that visually estimated winds and satellite scatterometer winds share similar characteristics, which are a function of stress rather than wind speed, and treat the estimated ship winds as equivalent neutral winds. Under such an assumption, we use statistical analyses to calculate the bias correction for estimated ship winds. Because observation practices vary by country and data provider, ICOADS identifies datasets by “deck” which is a number that allows for differentiating the source of the records (different deck numbers indicate different data collections provided to ICOADS, each which may contain one or more sources/countries). Three ICOADS decks 792, 926, and 992 contain the vast majority (~90%) of collocated visually estimated ship winds covering the time period November 1999-October 2009. The Root-Mean-Square difference between these visually estimated ship winds and scatterometer winds are 3.0ms^{-1} , 2.8ms^{-1} and 2.9ms^{-1} for each major deck respectively. Following the methodology of Freilich (1997) and Freilich and Dunbar (1999), we numerically show that for lower wind speeds (0ms^{-1} - 5ms^{-1} in this case) that the random error in the component of the visually estimated ship winds causes an artificial appearance of an overestimation relative to satellite scatterometer winds. We also extend this statistical artifact test to test higher wind speeds (12ms^{-1} - 18ms^{-1} in this case) through a Monte Carlo approach. An apparent slight drop of the conditional sample means relative to reference line is shown to be a statistical artifact. These artificial biases are properly accounted in this study. A new bias correction, LMS correction, is calculated and also compared to prior corrections such as Lindau (1995). This new bias correction is available for wind speeds ranging from 0ms^{-1} to 17ms^{-1} , because there are too few spatial and temporal collocated matches at wind speed greater than 17ms^{-1} . We are limited in our ability to perform the adjustments required for intercalibration because when comparing visual winds to scatterometer winds the necessary wind speed observations are rare and small in magnitude.

CHAPTER 1

INTRODUCTION

The Beaufort wind scale, devised in 1805 by Sir Francis Beaufort, is used by seamen and coastal observers to estimate wind speed. It includes 13 classifications (0 to 12) that describe various wind conditions. Initially, the 13 classes did not refer to wind speed but the sails behavior of a frigate, which is related to qualitative wind conditions. In 1900s, the descriptions were changed from how the sails behaved to how the sea behaved. It is notable that Beaufort scale is based on the visual and subjective observation of the sea surface condition, which is not an exact and objective scale. The estimated numeric wind speed for a given Beaufort value is usually determined from the midpoint value of the corresponding wind speed range. However, different observer could estimate different wind speed, even based on the same sea surface condition and practice. For more than a century, marine meteorologists have attempted to design a precise conversion of the Beaufort estimates scale into numeric wind speed. Many have developed Beaufort equivalent scales — WMO1100 (WMO 1970), CMMIV (WMO 1970), UWM (daSilva et al. 1995), Lindau (1995), Isemer (1992), Kaufeld (1981), Cardone (1969)— which were compared in Kent and Taylor (1997). According to Lindau (1995), any Beaufort equivalent scale should consider the universal relationship between the Beaufort force and the wind speed. This can be achieved through an orthogonal regression with an equal error variance in both the independent variable and dependent variable. Most of the previously published Beaufort equivalent scales cannot be described as equivalent scales due to the fact that they do not account for the different structures of error variances. This is because in one-way regression, either the variance of wind measurements or the variance of the Beaufort estimated winds are minimized. Of the Beaufort equivalent scales compared, the WMO 1100 conversion is the most commonly used in International Comprehensive Ocean-Atmospheric Data Set (ICOADS), but it is biased because it applies one-way regression to calculate the equivalent scales. In other words, the regressions are either regression of Beaufort force on the wind speed or the opposite regression of the wind speed on each Beaufort force. Alternatively, Kent and Taylor (1997) found that the Beaufort scale derived by Lindau, which has a more rigorous derivation and a

distribution closest to the distribution of the anemometer winds (slope=0.98, offset=-0.17ms⁻¹), is preferred.

ICOADS is considered to be the most complete and extensive archive of historical in situ marine meteorological observations available. Changing measurement technologies, such as more merchant ships equipped with anemometers and larger ships with anemometers at greater heights, have resulted in a reduction in estimated winds and caused a spurious increasing trend in the climate wind speeds (Ramage, 1987; Wright, 1988; Thomas et al., 2008). These technological changes have had a physically and statistically significant effect on the accuracy of wind measurements, if they are assumed to correspond to the WMO-mandated winds at a height of 10m above the surface (Thomas et al., 2008). ICOADS began in the United States and has grown to be what is currently the most comprehensive international dataset, incorporating a variety of observations from numerous countries and different research groups. Over the years, many significant contributions have been made to the ICOADS (e.g. the UK Met Office and NOAA Climate Data Modernization Program (CDMP) [Dupigny-Giroux et al., 2007] provided digitized and quality-checked data from logbooks (Woodruff et al., 2011)). Unfortunately, the changing measurement technologies, the multiple archive sources, and many significant historical events mean that ICOADS is not uniform to a wide range of users. To enhance its homogeneity, an ICOADS value-added database (IVAD) is being developed and will be implemented following the release of ICOADS Version 3.0 (anticipated May 2016). This will result in an advanced version of ICOADS, which will be accessible to the wider research community with recommended adjustments. The IVAD will add missing metadata (e.g., anemometer heights) and adjustments to the existing dataset, including adjustments to the WMO-mandated standard of 10m above the ocean surface (technically, above the displacement height, but this is assumed to be equal to the ocean surface). These adjustments are designed to remove systematic errors in the dataset (e.g., bucket observations of sea temperature could be adjusted to a skin temperature). In the future, the IVAD project will provide embedded bias adjustments for observation systems, with advanced quality control and improved uncertainty estimations.

To achieve the goals of intercalibration and adjustment, scientists around the world have been pooling their resources and sharing their collective thoughts. The IVAD project at FSU has focused mainly on calculation of the bias adjustments for visually estimated ship winds from

ICOADS and on creating a prototype of an IVAD attachment with the recommended adjustments. The FSU component of this project involves the adjustment of winds to a 10m wind on the same scale as satellite winds. The goal of this study is to improve the conversion of Beaufort estimated winds to geophysical values with scientific units (ms^{-1} in this case). This study specifically focuses on the adjustments to visually observed ship winds. In many ways, these winds are easier to adjust to satellite winds than anemometer winds; conversions to wind speed at a height of 10m have already been developed and estimated 'winds' are sensitive to variability in the form of a stress rather than an anemometer measurement. That is, they are winds relative to surface ocean currents and, given a stress (or a friction velocity), can be neutrally adjusted to a height of 10m, similar to the characteristics of satellite winds. Satellite winds are presently the best intercalibrated winds available (able to identify regional trends in the mean of $10\text{ms}^{-1}\text{decade}^{-1}$). Thus, we adjust to that standard even though satellite winds are equivalent neutral winds (Kara et al. 2008) as opposed to actual winds. Equivalent neutral winds are explained in Chapter 2.

Freilich (1997) applied a statistical artifact test at lower wind speeds to identify ranges affected by random component errors when one dataset is tuned to another dataset. Here, according to the argument from previous work (Freilich, 1997; Freilich and Dunbar, 1999), the author use Monte Carlo simulation to test the artificial bias at both high and low wind speeds. The results (Chapter 4) indicate that the random component error has a physically and statistically significant effect at lower wind speeds but only a small effect at higher wind speed.

The rest of the paper is organized as follows: Two datasets (ship winds and satellite scatterometer winds) in this study, including quality control (QC) and equivalent neutral wind, are described in Chapter 2. Chapter 3 introduces the methodologies involved in this project. Results and discussions, which resulted in a new bias correction for visually estimated ship winds, are described in Chapter 4.

CHAPTER 2

DATA

Two types of wind datasets are used in this study: visually estimated ship wind speed data from ICOADS Release 2.5 (Woodruff et al., 2011) and scatterometer wind speed data from the version 3 JPL QuickSCAT dataset. Location and position within each dataset are also used to collocate the wind observations.

2.1 ICOADS visually estimated ship wind speed dataset

The ICOADS R2.5 (NCDC, 1984; <http://rda.ucar.edu/datasets/ds540.0/>) has 261 million records in the International Maritime Meteorological Archive (IMMA) format, covering the time period 1662-2007 with a real time extension through present month (2008-present). Initial data analysis in this study focuses on the time period 1970-2007, in order to correspond with the marine air temperature adjustments developed by the National Oceanography Center (Berry et al., 2004). Our goal in this study is to develop an estimated ship wind speed adjustment to be provided as an *ivad* attachment in the IMMA format for each ICOADS record, and eventually embedded into an advanced version of ICOADS (ICOADS R3.0).

The reports in ICOADS are supplied by volunteer observing ships (VOS) and other platforms such as moored and drifting buoys. In this paper, we consider only those records from ships, which include the following platform types (PTs) as categorized by ICOADS: merchant ships or foreign military (PT=1); ocean station vessels, off station or station proximity unknown (PT=2); ocean station vessels, on station (PT=3); lightships (PT=4), or ships (PT=5). Other data records from non-ship platform are excluded, these are the following: US Navy or ‘deck’ log, or unknown (PT=0), moored buoy (PT=6), drifting buoy (PT=7), ice buoy (PT=8), ice station (manned, including ships overwintering in ice) (PT=9), oceanographic station data (bottle and low-resolution CTF/XCTD data) (PT=10), mechanical/digital/micro bathythermograph (MBT)(PT=11), expendable bathythermograph (XBT) (PT=12), Coastal-Marine Automated Network (C-MAN) (NDBC operated) (PT=13), other coastal/island station (PT=14), fixed ocean platform (PT=15), tide gauge (PT=16), high-resolution Conductivity-Temp.-Depth (CTD)/Expendable CTD (XCTD) (PT=17), profiling float (PT=18), undulating oceanographic

recorder (PT=19), autonomous pinneped bathythermograph (PT=20) or glider (PT=21) (Woodruff et al., 2015).

In ICOADS, wind speed indicator (WI) represents the method of wind observation. If known, it is provided by the wind speed indicator flag, which indicates the original units (knots, ms^{-1} , or Beaufort Force) and whether the wind was estimated or measured. This study uses all reports associated with visually estimated ship wind from ICOADS R2.5; in other words, all records from ships with a WI that defines the wind speed as “estimated” (i.e., WI = 0 (Meter per second, estimated), 2 (Estimated (original units unknown)), 3 (Knot, estimated), 5 (Beaufort force (conversion of original data or based on documentation)), or 6 (Estimated (original units unknown) or unknown method)) (Woodruff et al., 2015). One of these values is ambiguous, WI=6, which indicates the method is estimated or unknown (Slutz et al., 1985). For this study, we assume that most of the ambiguously flagged reports were estimated and thus assign all data with this flag to the estimated winds (similar to Thomas et al., 2008). Those records with a WI that defines the wind speed as “measured” are excluded (i.e., WI=1 (meter per second, obtained from anemometer (measured)), 4 (knot, obtained from anemometer (measured)), 7 (measured (original units unknown)), or 8 (high-resolution measurement (e.g. hundredths of a meter per second))) (Woodruff et al., 2015).

All the visually estimated ship winds in IMMA format are extracted from ICOADS R2.5 covering the time period 1970-2007. Initially, we expected all visually estimated ship winds to fall into categories the same as those in the Beaufort scale, which categorizes wind speed values into 13 discrete bins allowing the Lindau scale to be directly applicable to all visually estimated ship wind. However, only ship winds with WI=5, commonly referred to as Beaufort winds, approximate the ‘13 value’ distribution with those smaller peaks (Figure 1). Because observation practices vary by country and data provider, ICOADS identifies datasets by “deck” which is a number that allows for differentiating the source of the records (different deck numbers indicate different data collections provided to ICOADS, each which may contain one or more sources/countries). The search for this period reveals only two decks (761 - Japanese Whaling Ship Data (CDMP/MIT digitization, 1946-1984 and 792 - US National Centers for Environmental Prediction (NCEP) BUFR GTS: Ship Data) with WI=5 records. Since the majority of these observations came from deck 761 (4,257 observations vs 9 for deck 792), the distribution of the wind speeds with WI=5 are categorized by this deck determined that the

Lindau's (1995) scale can be applied to deck 761 for the prototype *ivad* attachment. Figure 3 shows the distribution of wind speed for deck 761 with WI=5. The figure illustrates a '13 value' distribution with 12 discrete peaks from force 0-11 (force 12 observations are very rare and thus were not observed). This indicates the original Beaufort values use the WMO 1100 scale (Simpson 1906), which is the most commonly used Beaufort equivalent scale in ICOADS.

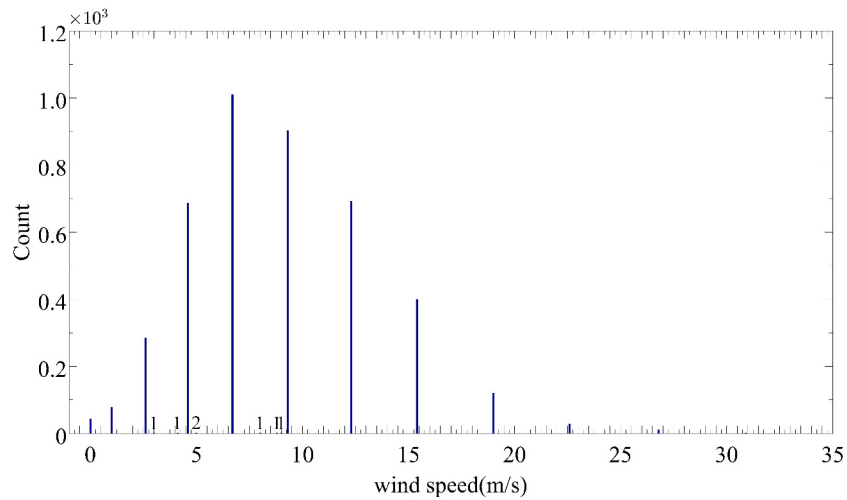


Figure 1. Histogram of wind speed with WI=5, for ships only. The counts of smaller peaks are labeled.

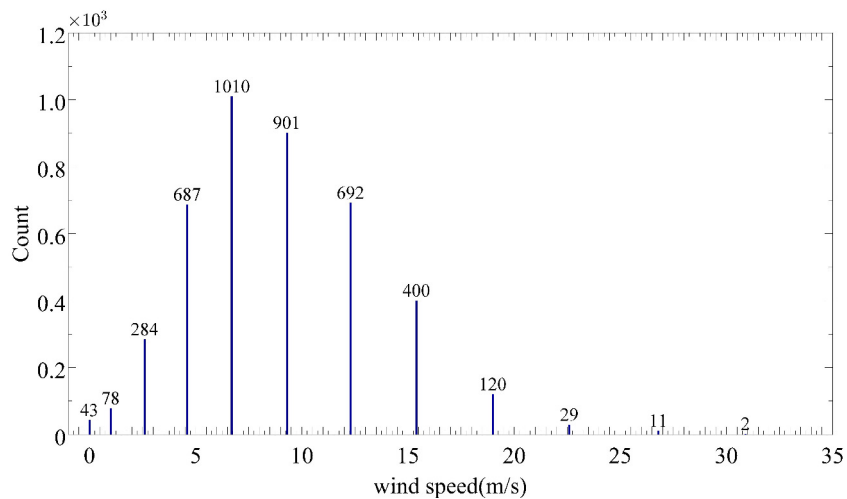


Figure 2. Histogram of wind speed with WI=5 with deck 761. The count of each peak is labeled.

Applying the Lindau (1995) scale is a straightforward process that involves comparing 13 wind speed values in Lindau (1995) scale to the values of wind speed with WI=5 for deck 761 (Table 1). According to Lindau (1995), the corrected value should be this new value obtained by

applying the Lindau scale; this corrected value should replace the existing wind speed value in ICOADS. Therefore, Lindau's (1995) correction value is the difference between the Lindau (1995) scale and the WMO 1100 scale as shown in the bottom row of Table 1.

However, distribution of wind speed values with WI=0, 3 and 6 (Fig. 4a, b, and c) shows a more scattered wind distribution. WI=2 is not shown in this study due to the limited number of reports available.

Because of the varied national observation practices, the following histograms of wind speed distribution (Fig. 5, 6, and 7) for WI= 0, 3, and 6 respectively are categorized by major decks and illustrate that wind speed values fall into more discrete bins than the 13 bins associated with the Beaufort scale. In Figure 5a, it is shown that deck 732 had many more observations at 0ms^{-1} and 4ms^{-1} than in the other wind speed values. Whereas in Figure 5b, the wind speed values from deck 792 show (1) fewer observations at 0ms^{-1} as compared to other wind speed values, and (2) wind speed observations at 5ms^{-1} are the most prevalent in this dataset. Figure 5c shows a very different wind speed distribution for deck 888 with upward of 20 or more primary peaks and numerous smaller secondary peaks. It is notable that many of the visual reports have a similar structure with 2 or more small peaks for every large peak in Figure 5c. This can be attributed to the differences in observation practices.

Table 1. Applying the Lindau's (1995) scale. Lindau (1995) values are converted to ms^{-1} by multiplying by 0.5144 and rounding to one decimal place. Deck 761 contained no wind speeds associated with Beaufort force 12.

BFT	WMO 1100/WI=5, deck 761 (ms^{-1})	Lindau (1995; ms^{-1})	Lindau's (1995) correction (ms^{-1})
0	0.0	0.0	0.0
1	1.0	1.2	-0.2
2	2.6	2.7	-0.1
3	4.6	4.6	0.0
4	6.7	7.2	-0.5
5	9.3	9.7	-0.4
6	12.3	12.1	0.2
7	15.4	14.6	0.8
8	19.0	17.2	1.8
9	22.6	20.2	2.4
10	26.8	23.4	3.4
11	30.9	27.1	3.8
12	--	31.4	--

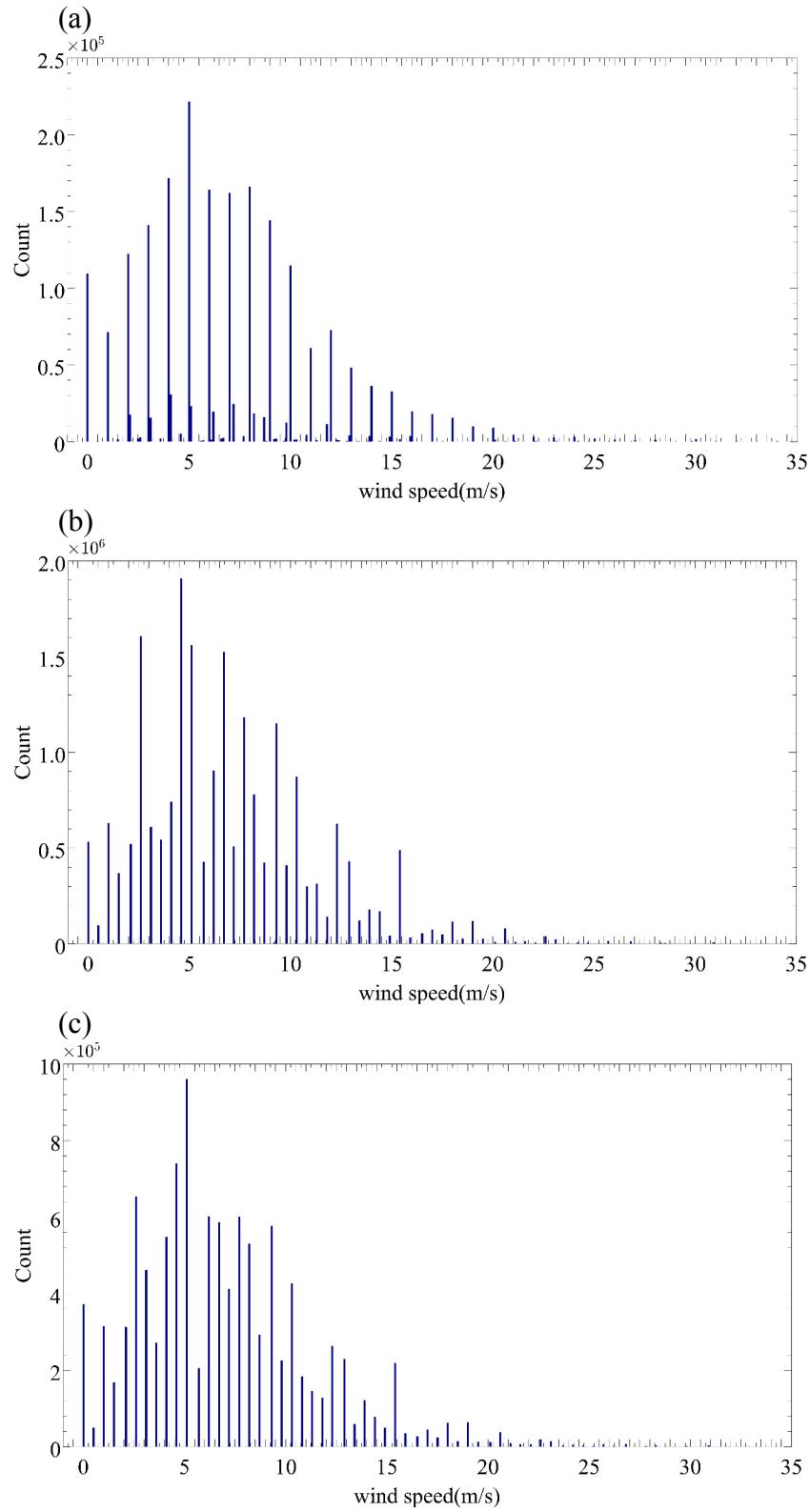


Figure 3. Histogram of wind speed with (a) WI=0 (Meter per second, estimated; (b) WI=3 (Knot, estimated); (c) WI=6 (Estimated (original units unknown) or unknown method)).

While all observers are instructed to give an upper and lower limit plus a mid value, the various countries and data providers handle this differently. For instance, the instructions given to US observers have slightly different midpoints than the instructions given to UK observers. This results in the appearance of some smaller peaks grouped closely together. Figures 5d and 5e show wind speed observations for decks 926 and 892, but, unfortunately, datasets from these two decks do not display the expected ‘13 value’ distribution as well. It is found that the histograms of wind speed distribution with WI=3 and WI=6 for each major deck are similar to those with WI=0 (Figure 5) in that they reveal a less sparsely filled wind speed distribution than the anticipated ‘13 value’ distribution.

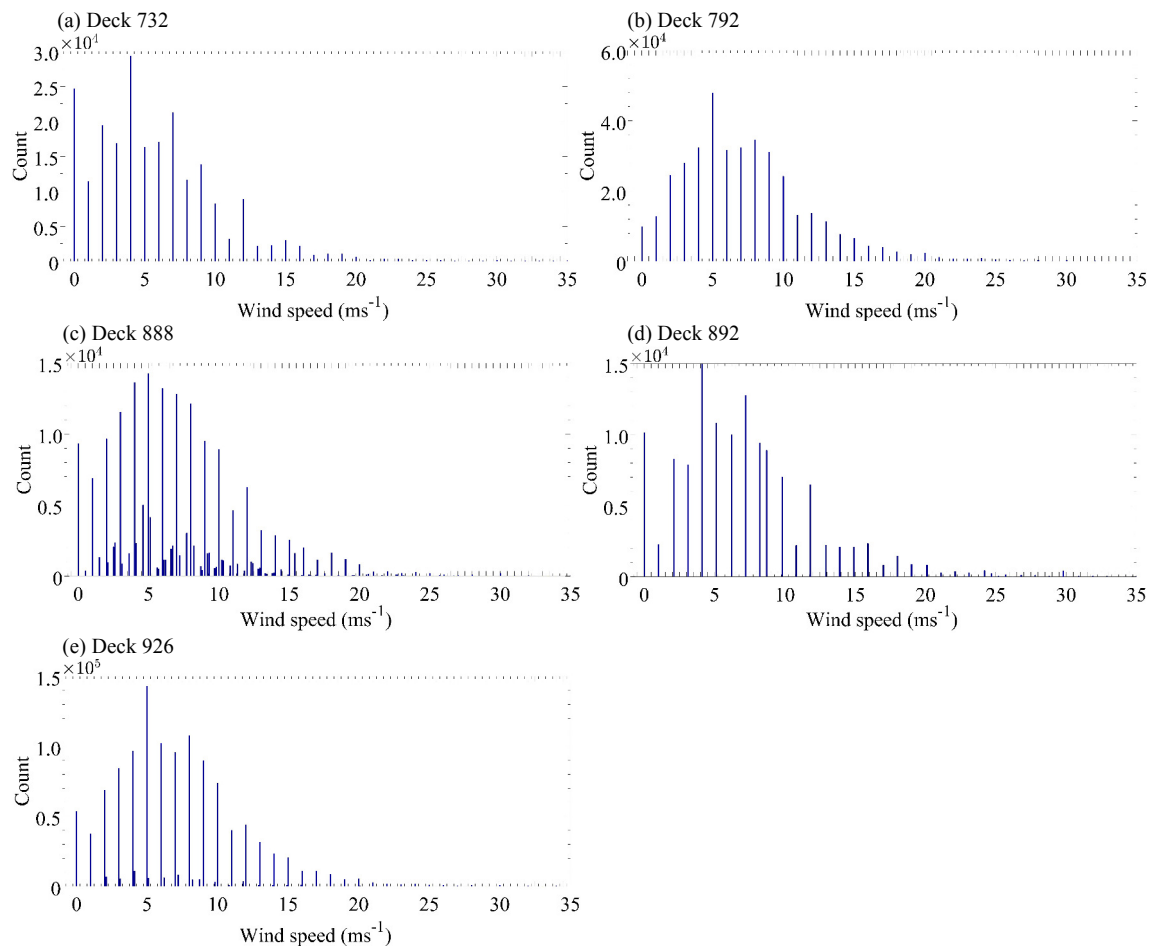


Figure 4. Histogram of ship wind speed with WI=0 categorized by major decks. (a) Deck 732: Russian Marine Met. Data Set (MORMET) (rec’d at NCAR). (b) Deck 792: US National Centers for Environmental Prediction (NCEP) BUFR GTS: Ship Data. (c) Deck 888: US Air Force Global Weather Central (GWC). (d) Deck 892: US National Centers for Environmental Prediction (NCEP) Ship Data. (e) Deck 926: International Maritime Meteorological (IMM) Data.

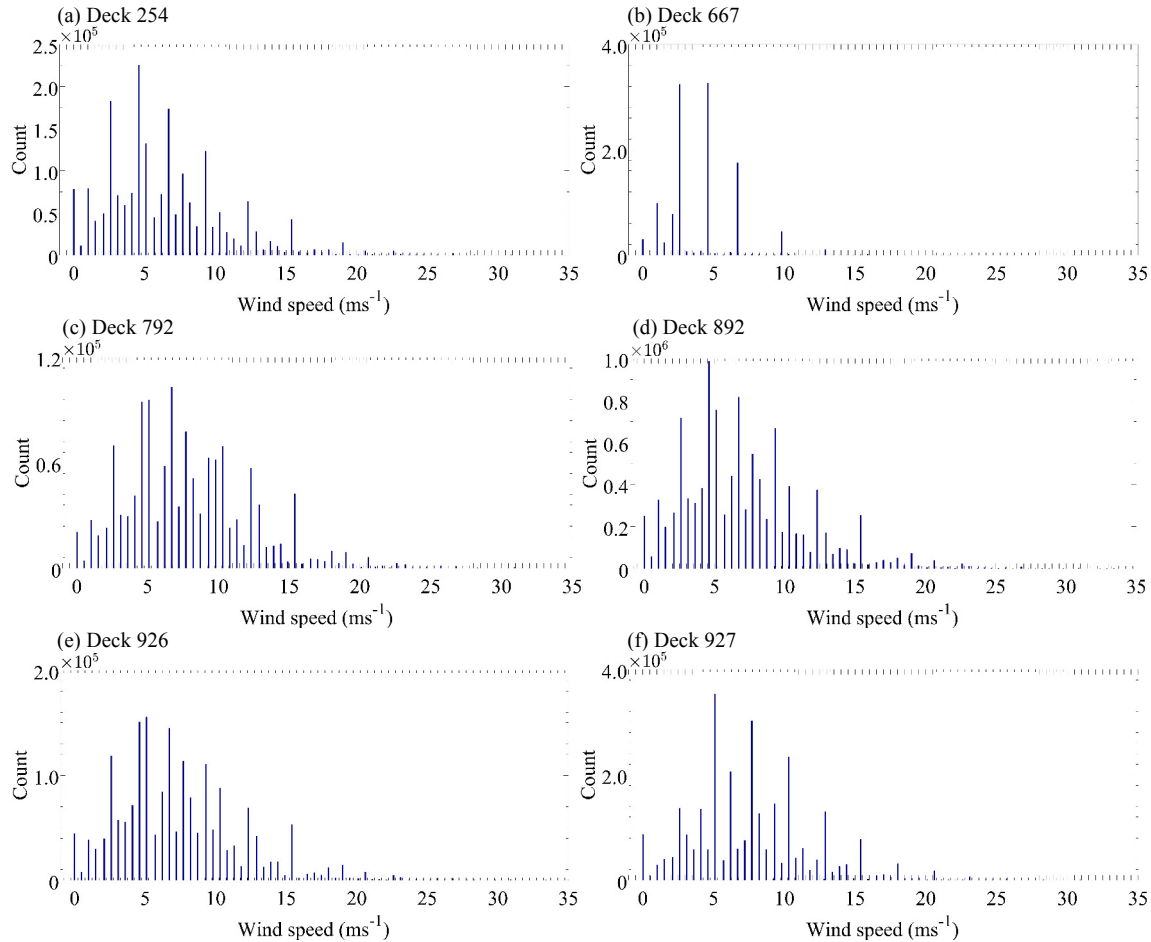


Figure 5. Histogram of wind speed with WI=3 categorized by major decks. (a) Deck 254: UK Met. Office (MetO) Main Marine Data Bank (MDB). (b) Deck 667: Inter-American Tropical Tuna Commission (IATTC). (c) Deck 792: US National Centers for Environmental Prediction (NCEP) BUFR GTS: Ship Data. (d) Deck 892: US National Centers for Environmental Prediction (NCEP) Ship Data. (e) Deck 926: International Maritime Meteorological (IMM) Data. (e) Deck 927: International Marine (US-or foreign-keyed ship data, 1970-2007)

As previously mentioned, we expected all visually estimated ship winds to fall into categories the same as those in the Beaufort scale. However, reviewing the histograms makes it clear that identifying actual Beaufort winds (outside of WI=5) within the ICOADS records is challenging and the application of Lindau scale on all visually estimated ship winds is problematic. This can be explained by the fact that in many cases, as a result of observer subjectivity or varying observation practices, no documentation or valid information exists to confirm which Beaufort scale the observers used and how they converted it to numeric wind speed. Because different countries and data providers use different Beaufort scales and vary in their instructions to observers, the Lindau (1995) correction is not applicable. The 13 values of Lindau’s (1995) correction would force too much data to be excluded.

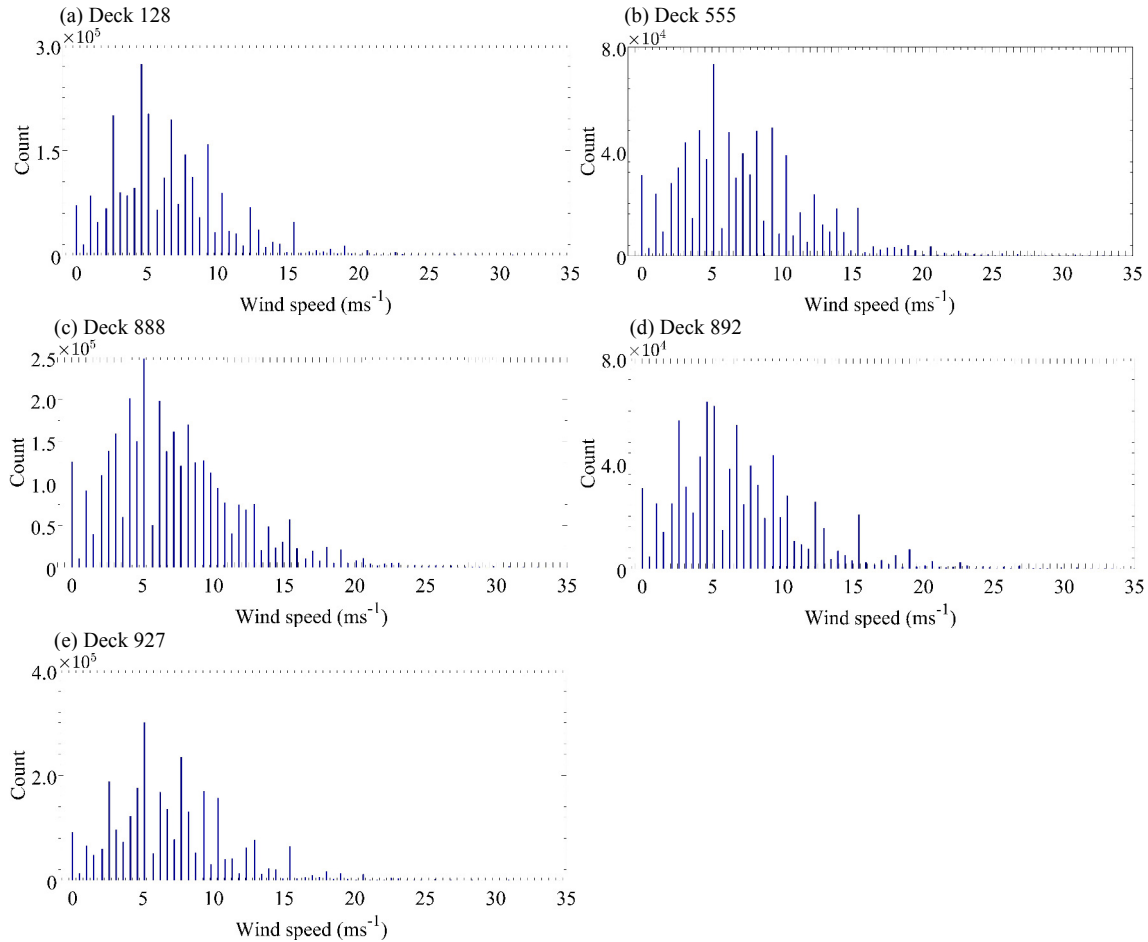


Figure 6. Histogram of wind speed with WI=6 categorized by major decks. (a) Deck 128: International Marine (US-or foreign-keyed ship data; 1950-1978). (b) Deck 555: US Navy Fleet Numerical Meteorology and Oceanography Center (FNMOC; Monterey) Telecom. (c) Deck 888: US Air Force Global Weather Central (GWC). (d) Deck 892: US National Centers for Environmental Prediction (NCEP) Ship Data. (e) Deck 927: International Marine (US-or foreign-keyed ship data; 1970-2007).

2.2 Scatterometer wind speed dataset

The Jet Propulsion Laboratory’s QuikSCAT Level 2B (L2B) Version 3 dataset (SeaPAC, 2013) contains the latest reprocessed version of Level 2B ocean surface wind vector retrievals from the QuikSCAT scatterometer, with a non-uniform grid at 12.5km pixel spacing within the observational swath. This dataset is stored in NetCDF format and covers approximately 90% of the global oceans (ice-free) daily. Several improvements were made in Version 3 (Fore et al., 2014) as compared to the previous JPL processing of the QuikSCAT L2B wind speed dataset. The JPL QuikSCAT version 3 improvements include:

“(1) Changes to measurement binning that decrease noise and other seemingly random errors and to reduce gaps in the 12.5 km L2B wind retrievals.

(2) An improved geophysical model function (GMF) to model the effect of wind on backscatter.

(3) A neural network approach to correct rain contaminated wind speeds.

(4) Estimation and removal of cross-track dependent wind speed biases from the wind retrievals. The 12.5 km binning resolution enables users to obtain wind vector retrievals 10 km closer to shore when compared to the 25 km L2B dataset (only available in versions 1 and 2).” (JPL, 2013)

These improvements provide us with more potential collocated matches for intercalibration purposes and improve the quality of the dataset with less rain contamination, closer collocation and a less of a mismatch in sampling volume between in situ and satellite data.

2.3 Equivalent neutral wind

The actual wind speed is approximately logarithmically proportional to the height above local sea level. In this log-profile, the atmospheric stability plays a significant role. As such, the wind profile can be written as

$$U(z) - U_s = (u_* / k) \ln(z / z_0) + (u_* / k) \varphi(z, z_0, L) \quad (2.3.1)$$

Where U is the wind speed as a function of height (z), U_s is the wind speed at the ocean surface, u_* is the square root of the kinematic stress (parallel to $\mathbf{U} - \mathbf{U}_s$), and k is the von Kármán constant. φ is the stability function for momentum (zero for neutral condition in this study), L is the Monin–Obukhov length, and z_0 is the roughness length for momentum.

Satellite scatterometer winds are calibrated to equivalent neutral winds (Liu and Tang, 1996; Verschell et al., 1999; Mears et al., 2001) rather than actual wind speeds regarding to the atmospheric stratification. In the most commonly preferred definition (Ross et al., 1985; Liu and Tang, 1996; Verschell et al., 1999), the equivalent neutral wind is only related to the stress and roughness length consistent with the observed atmospheric stratification (Kara et al., 2008), but the atmospheric stratification term in the modified log-wind profile is set to zero. This definition is consistent with scatterometry, which is more stress-like than wind-like. This is because that by sending microwave to the ocean surface from scatterometer and measuring the strength of

backscatter signal, the backscatter signal power is responding to the surface waves or ripples (i.e., surface roughness), which are equilibrium with the wind stress (Liu and Tang, 1996). Therefore, the equivalent neutral winds are defined as follows:

$$U_{10EN} = (u_* / k) \ln(10 / z_0) \quad (2.3.2)$$

where u_* and z_0 are calculated beforehand considering atmospheric stratification and the surface current.

The scatterometer and visual observations are all based on surface stress observations. Because we lack the information to account for stability-related modifications to the adjustment from the surface to 10m, a neutral adjustment is used. For this study, we treated the visually estimated ship winds as equivalent neutral winds and evaluate the accuracy of this assumption.

2.4 Quality control

Quality control (QC) has been applied to the QuickSCAT scatterometer wind speed dataset and ICOADS R2.5 visually estimated ship wind dataset respectively by removing the poor quality data using QC flags provided with each respective dataset.

QuickSCAT is a Ku-Band (13.4 GHz/2.24 cm) microwave scatterometer that measures the ocean surface roughness. The Ku-band scatterometer can be sensitive to rain contamination (Weissman, 2012) under some wind and rain conditions. These errors in wind retrieval occur because of the scattering and absorption of the transmission energy of the scatterometer (Draper and Long 2004); changing ocean surface roughness by the rain (Sobieski et al. 1999; Weissman, 2008); and, energy backscattered from rain (Weissman, 2008). Rainflags have been developed for QuickSCAT (Portabella and Stoffelen, 2001; Huddleston and Stiles, 2000; Boukabara et al., 2002) to identify those data with rain contamination and these rain flags appear to work well (Hoffman et al., 2004) for calibration purposes, meaning that they aggressively remove data that might be rain contaminated. One problem with this approach is that very strong winds are often accompanied by rain (JPL, 1999). To improve the quality of datasets, based on recommendations from these previous works, all rain flagged scatterometer data have been removed from this study.

For ship winds, each record in the ICOADS R2.5 contains an *Icoads* attachment, which contains one of QC elements denoted as ‘WNC’ flags. To improve the quality of dataset for

calibration purposes, each ICOADS record extracted with a WNC flag denoted as 'erroneous' is excluded.

CHAPTER 3

METHODOLOGIES

Following a thorough examination of wind values denoted as “estimated” in ICOADS, the author determined that a new bias correction could be calculated by comparing satellite scatterometer winds and collocated visually estimated ship winds. Due to the sensitivity of the SeaWinds scatterometer on the QuickSCAT to ocean surface changes, satellite scatterometer winds are calibrated to equivalent neutral winds (Liu and Tang, 1996; Verschell et al., 1999; Mears et al., 2001) rather than actual wind speeds. The conversion from actual wind to equivalent neutral winds is widely accepted, assuming additional information is available: SST, air temperature, humidity, surface pressure, stress or sea state, and surface current. Previous work (e.g. Bourassa et al., 2003 *JGR*; May and Bourassa, 2010) showed that QuickSCAT winds are very accurate, with root-mean-square (rms) differences between the datasets of roughly 1ms^{-1} . This difference represents an upper bound on the uncertainty; with some of the differences coming from errors in buoy data and from mismatches in the spatial/temporal scales of buoy and satellite data (Stoffelen, 1998). In this study, ship-estimated winds are presumed to be sensitive to geophysical variability in the same manner as equivalent neutral winds. This is supported by the results of our comparison and these results will allow a satellite-like wind climatology to be extended back in time (for decades) in the data rich areas (e.g., the North Atlantic Ocean).

3.1 Collocation between satellite scatterometer winds and visually estimated ship winds

The key properties of collocation are:

1. Time threshold: 30min (1800s);
2. Distance threshold: 25km.

The steps for the collocation are:

1. Finding all data matches within 30 minutes of each other;
2. Of the data matches found in step 1, identifying the ones that match in space within 25km;
3. Of the data matches found in step 2, finding the closest match in space.

We limited the temporal and spatial window to 30 min and 25 km respectively in order to obtain the necessary number of high quality collocated comparison matches. By using the above space/time procedure to find the closest spatial match, we can deduce the systematic error in the inter-calibration between the satellite scatterometer winds and collocated estimated ship winds.

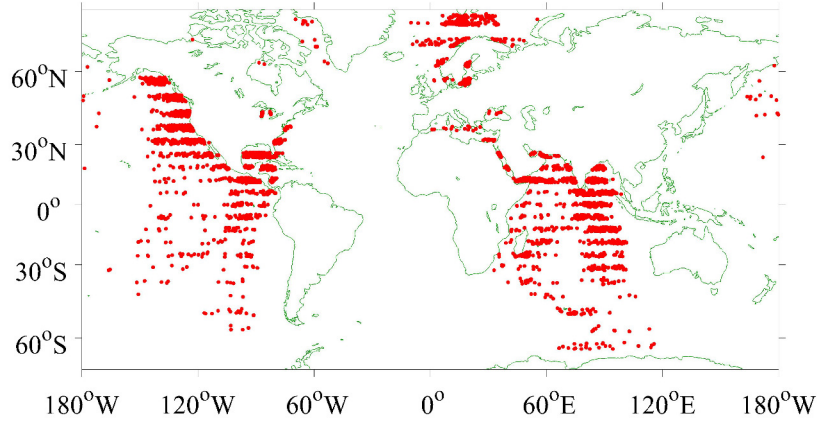


Figure 7. Map for collocated estimated ship winds. Red dots are associated with location of collocated estimated ship winds. The limited spatial sample is related to the satellite coverage at the times of day of the ship observations.

3.2 Modification of the calibration due to statistical artifacts

Freilich and Dunbar (1999) and Freilich (1997) used buoy data and scatterometer data to show that noise in one dataset can cause the appearance of a bias at lower wind speeds (0ms^{-1} to 3ms^{-1}). Freilich (1997) numerically examine this problem by treating a buoy dataset as error-free dataset (including intercalibrated with the satellite dataset) and adding noise to it to match the distribution of data in the satellite dataset. They found that the appearances of artificial biases occur near the boundaries of the parameter (specifically a wind speed of 0ms^{-1}). This is because that a data density shift occurs near the lower boundary of wind speed. Because of the nonnegative constraint on the wind speed, the artificial bias causes those combined vector components negative values to change to positive values. This problem could also occur where there is a very large shift in data density due to the noise, which is similar to a boundary.

In Freilich's (1997) model, the noisy vector wind speed can be numerically simulated as an error-free observation (i.e., perfectly inter-calibrated) plus random noise for each of the vector components, such that

$$S_{mi} = [(S_i \cos \theta_i + \delta_i)^2 + (S_i \sin \theta_i + \delta_i)^2]^{1/2} \quad (3.2.1)$$

Where δ is normal distributed random noise, θ is uniformly distributed wind direction,

s_{ni} is *ith* the noisy wind speed, and s_i is the *ith* noise-free wind speed; Random error can cause sign changes in the components of the vector. However, under nonnegative constraint (e.g., Eq. 3.2.1) on the wind speed, vector components are always combined to determine a positive wind speed. When paired data are binned in terms of one dataset, the result is that the average value of the other dataset increases near a boundary. We are dealing with paired data for which error is added to only one of the pair, and we are binning according to the data to which errors have been added. Errors that reduce the value used in sorting cause the unmodified value of the paired data to be added to a lower bin, resulting in an overestimation at that wind speed. If the unmodified data are uniformly distributed and away from a boundary, these biases are cancelled out by symmetric noises (like number of data points moved in each direction along the number line). Near boundaries, the shifts towards the boundary are not compensated and the binned average of the paired and unmodified data near a lower boundary is greater than expected from the data used for sorting. Therefore, there is the false appearance of a bias near the lower boundary, with the magnitude of the apparent bias and the range of which there are substantial biases dependent on the noise of the data used to sort (i.e., the data on the x-axis). These biases are called false biases because they can be explained by random error in the data.

This leads to the calculation of sample conditional means of the y-axis variables for each bin, that might not match the x-axis values. Sample conditional means of the y-axis mean, which are nonlinear functions of x-axis wind speed and the noise are not well described by a simple linear fit (e.g., linear correlation), unless the noise in the x-axis variable is small. The biases found in this type of comparison allow us to calculate the artificial effect of the random component error on biases near a boundary.

3.3 Assessment of systematic errors as a function of wind speed

When considering the slope, if the error/noise variance in both variables to be regressed is not equal, the effect of the error/noise on the slope can be predicted (Kent and Taylor, 1997). Due to larger error/noise variance in the least accurate variable, the slope of the regression of the least accurate variable on the most accurate variable will be less underestimated than the slope of opposite regression (Kent and Taylor, 1997). The intercalibration assumes both wind speed data sets are unbiased. In the case of a least squares best fit (equation 3.3.1), the slope is only related to the covariance of both data sets (which is influenced by noise) and the variance of the x-axis

data. This means that the noise on the x-axis (if large enough to be noticeable) has more influence than the noise on the y-axis. From a mathematical perspective, in the following formula¹ when flipping both axes (in other words switching the ‘x’ associated with the satellite scatterometer wind speed and the ‘y’ associated with the collocated visually estimated ship wind speed) the numerator is constant, whereas the denominator is dependent on the variance of noise in each wind speed dataset.

$$slope = \frac{\sum_{i=1}^n (x_i - \bar{x})(y_i - \bar{y})}{\sum_{i=1}^n (x_i - \bar{x})^2} = \frac{Cov[x, y]}{Var(x)} \quad (3.3.1)$$

Applying this form to the above discussion, we have:

$$slope_{scat} = \frac{Cov[w_{scat}, w_{ship}]}{Var(w_{scat})} > slope_{ship} = \frac{Cov[w_{ship}, w_{scat}]}{Var(w_{ship})} \quad (3.3.2)$$

Where $slope_{scat}$ denotes the slope of the linear fit line when the satellite scatterometer winds are plotted on the horizontal axis and the collocated estimated ship winds are plotted on the vertical axis, $slope_{ship}$ denotes the slope of the linear fit line when the satellite scatterometer winds are plotted on the vertical axis and the collocated estimated ship winds are plotted on the horizontal axis, w_{ship} denotes the collocated estimated ship wind speed dataset, and w_{scat} denotes the satellite scatterometer wind speed dataset. $slope_{scat}$ is greater than $slope_{ship}$, which indicates that the variance of noise in the scatterometer wind speed dataset is less than the variance of noise in the estimated ship wind speed dataset. This supports a conclusion that the satellite scatterometer wind speed dataset is much more accurate than the collocated estimated ship wind speed dataset. When dealing with paired data, the slope is most consistent when the noise variance in each variable is the same. When they are substantially different, it is best to plot the most accurate observations as independent variables and the least accurate observations as dependent variables. Under such conditions, the increased variance in the independent variable causes the artificial appearance of a bias.

¹ This formula is available from Wikipedia
(https://en.wikipedia.org/wiki/Simple_linear_regression)

3.4 Significance test

Statistical significance test is used to assess the statistical value of the bias adjustments that are calculated herein. In this study, we assume random error only, which is normally distributed. This technique can address the question: Is the difference between the bin of artificial error-free ship winds and satellite winds large enough to confidently be identified as a bias? This can be determined by the difference between the median of collocated ship winds and mean of satellite scatterometer winds within each 0.5ms^{-1} bin. It is used to examine if the biases in individual bins are statistically significant. To conduct the hypothesis test for the each bin, we use the two-tailed t-statistic, which follows a t-distribution; and the value of α is set to 0.01. If the calculated P-value is less than or equal to α , then it is “unlikely,” which indicates rejection of the null hypothesis, which is associated with the artificial bias can be confidently identified as a bias, and application of the bias correction. Otherwise it is “likely,” which indicates no bias adjustment needed.

CHAPTER 4

RESULTS AND DISCUSSION

This project compared satellite scatterometer wind speed data from version 3 JPL QuickSCAT to collocated ship winds data from ICOADS R2.5 by plotting the most accurate satellite winds as independent variables and the least accurate ship winds as dependent variables (Kent and Taylor, 1997). Since wind speed dataset from QuickSCAT was only available for the period November 1999 to October 2009, this comparison is limited to that time period. A search of the collocated data pairs (6,782 pairs) revealed three decks (792, 926, and 992) with a high frequency (~90%) of estimated wind observations:

1. Deck 700: UK Met. Office VOSclim GTS BUFR Data (2 observations).
2. Deck 792: US National Centers for Environmental Prediction (NCEP) BUFR GTS: Ship Data (2,404 observations).
3. Deck 874: Shipboard Environmental (Data) Acquisition System (SEAS) (223 observations)
4. Deck 926: International Maritime Meteorological (IMM) Data (3,098 observations).
5. Deck 927: International Marine (US- or foreign-keyed ship data) (55 observations)
6. Deck 992: National Climate Data Center (NCDC) GTS: Ship Data (1,000 observations).

Because of the varied national observation practices, we categorized the collocated match pairs between satellite scatterometer winds and estimated ship winds by these three decks (792, 926, and 992). Figures 9a, b and c show an apparent overestimation of collocated estimated ship winds to satellite scatterometer winds at the lower wind speeds in those three decks. The density contours indicate that wind speed ranging from 5ms^{-1} to 10ms^{-1} are the most common in this study; this is also consistent with the most frequently observed wind speed range in the real world. However, these density contours do not closely follow the linear-fit line, which demonstrates that the bias adjustments cannot be reasonably addressed by simple linear regression and different bias correction values for different ranges of wind speed may be needed. This is because the intercept of linear fit at the vertical axis can be explained by artificial bias,

which is a false appearance of bias and can be explained by purely random error in the vector component of wind speed.

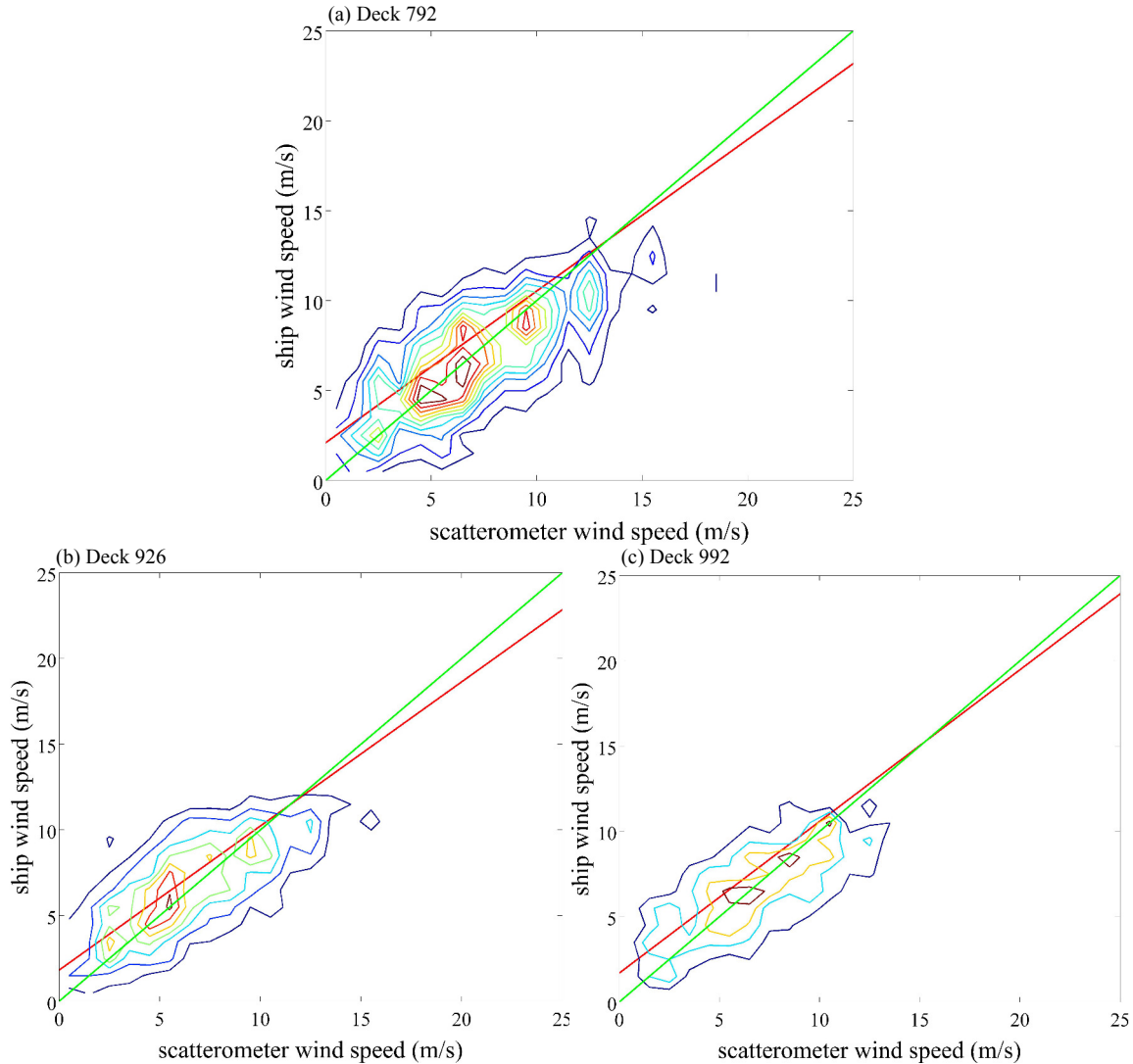


Figure 8. The density plot for the collocation wind speed scatter plot categorized by major decks for the period Nov. 1999-Oct. 2009. The contour line indicates density contours, which are associated with the number of data points fall into a $1\text{ms}^{-1} \times 1\text{ms}^{-1}$ box. The green line is reference line. The red line is the simple linear fit line. (a) Deck 792; (b) Deck 926; (c) Deck 992;

In addition, whisker boxplots are plotted for each deck in Figures 9a, b, and c. The common features of these three figures are (1) a large overestimation at low wind speeds of collocated estimated ship winds versus the scatterometer winds; and (2) collocated match pairs at higher wind speed area (e.g., in the range of 12ms^{-1} to 18ms^{-1}) are rarely found in the collocation, and most of wind speeds are distributed below 12ms^{-1} . The medians on these whisker boxplots

for wind speeds (greater than 5ms^{-1} for decks 792 and 992, and greater than 3ms^{-1} for deck 926) largely follow the reference line.

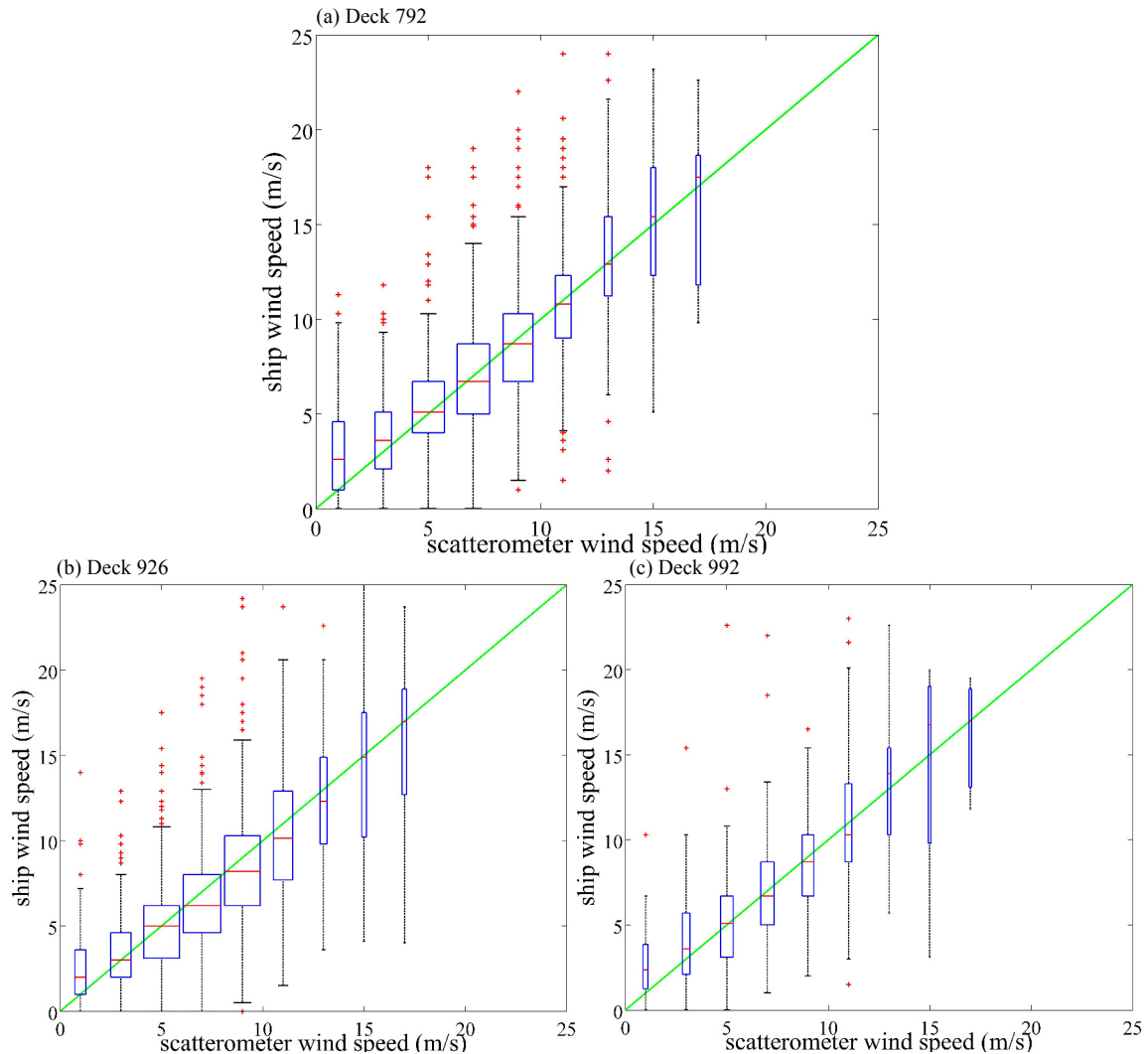


Figure 9. The boxplots for the three different decks (792, 926, and 992). Each of the whisker boxes is associated with the number of data points in a range of 2ms^{-1} of scatterometer wind speed. The width of each whisker box is proportional to the data points within each 2ms^{-1} bin. (a) Deck 792; (b) Deck 926; (c) Deck 992.

Freilich (1997) found a way to interpret this overestimation at lower wind speed by comparing the collocated buoy winds to the scatterometer winds. The author found that random error in the component of vector winds would significantly change the distribution of wind speed at lower wind speed area (0ms^{-1} to 3ms^{-1}), which can be considered to be artificial bias due to the non-negativity of wind speed. This false appearance of bias is often misrepresented as systematic calibration error. Therefore it is necessary to investigate the binned average within each 0.5ms^{-1} bin (conditional sample mean) near the lower boundary of wind speed in order to distinguish

artificial bias from systematic error. In cases such as this, the conditional sample mean of vector ship winds increases near the lower boundary within each 0.5ms^{-1} bin of the satellite scatterometer winds

Uncertainty estimation for each deck (792, 926 and 992) indicates the Root-Mean-Square (RMS) difference between satellite scatterometer winds and collocated ship winds are 3.0ms^{-1} , 2.8ms^{-1} and 2.9ms^{-1} , respectively. Therefore, we can numerically and statistically simulate the comparison between the scatterometer winds and collocated estimated ship winds for each major deck (792, 926, and 992) by generating a uniform distributed dataset, and adding noise following normal distribution to match the collocated ship winds. This technique is known as “histogram matching.”

In Figure 11, the data from decks 792 and 992 reveal close matches between the medians of boxplot and the black dots associated with conditional sample mean within each 0.5ms^{-1} bin. This provides us with an estimate of the artificial bias associated with random component error at the lower boundary of wind speed (0ms^{-1}). The data from deck 926 still shows that biases exist in that wind speed dataset (as displayed by the difference between the conditional means and the medians in each bin). This inconsistency in the analyses could be because of a non-uniform uncertainty across the dataset for deck 926. Investigation this complication would require much more detailed assessment of the data going into this deck, and how it differed from other decks.

Using the previous argument for testing low wind speeds, we can extend the artifact bias argument to test higher wind speeds (in this case, 14ms^{-1} to 20ms^{-1}), which depends upon the collocation between satellite winds and collocated ship winds.

Since the distribution of realistic winds does not follow the uniform distribution and there are relatively few observations for high wind speeds, we use Monte Carlo simulation to generate a new dataset to oversampling the scatterometer data at higher wind speed as error-free observation, and add noise to match collocated ship winds. This approach accounts for the realistic distribution of the wind speeds, and has not ever done before. By binning the wind speed to fall within 0.5ms^{-1} range of the error-free wind speed dataset (Figure 12a, b and c), the comparison between these two new datasets shows that 1) the conditional sample mean of the three decks falls off slightly from the reference line near the higher wind speed boundary (around 20ms^{-1}); and 2) the results at lower wind speeds is consistent with the previous statistical artifact

test. This result supports a conclusion that the artifact bias has a small effect on the changes in wind speed distribution at higher wind speeds, and a significant impact on the lower wind speeds.

It is notable that deck 792 and deck 992 are from two different data providers, with approximately 5% difference in their numbers, and their original data source are both from marine Global Telecommunication System (GTS). This similarity of source explains similarity in the comparison of satellite scatterometer winds to the collocated estimated ship winds for each two decks.

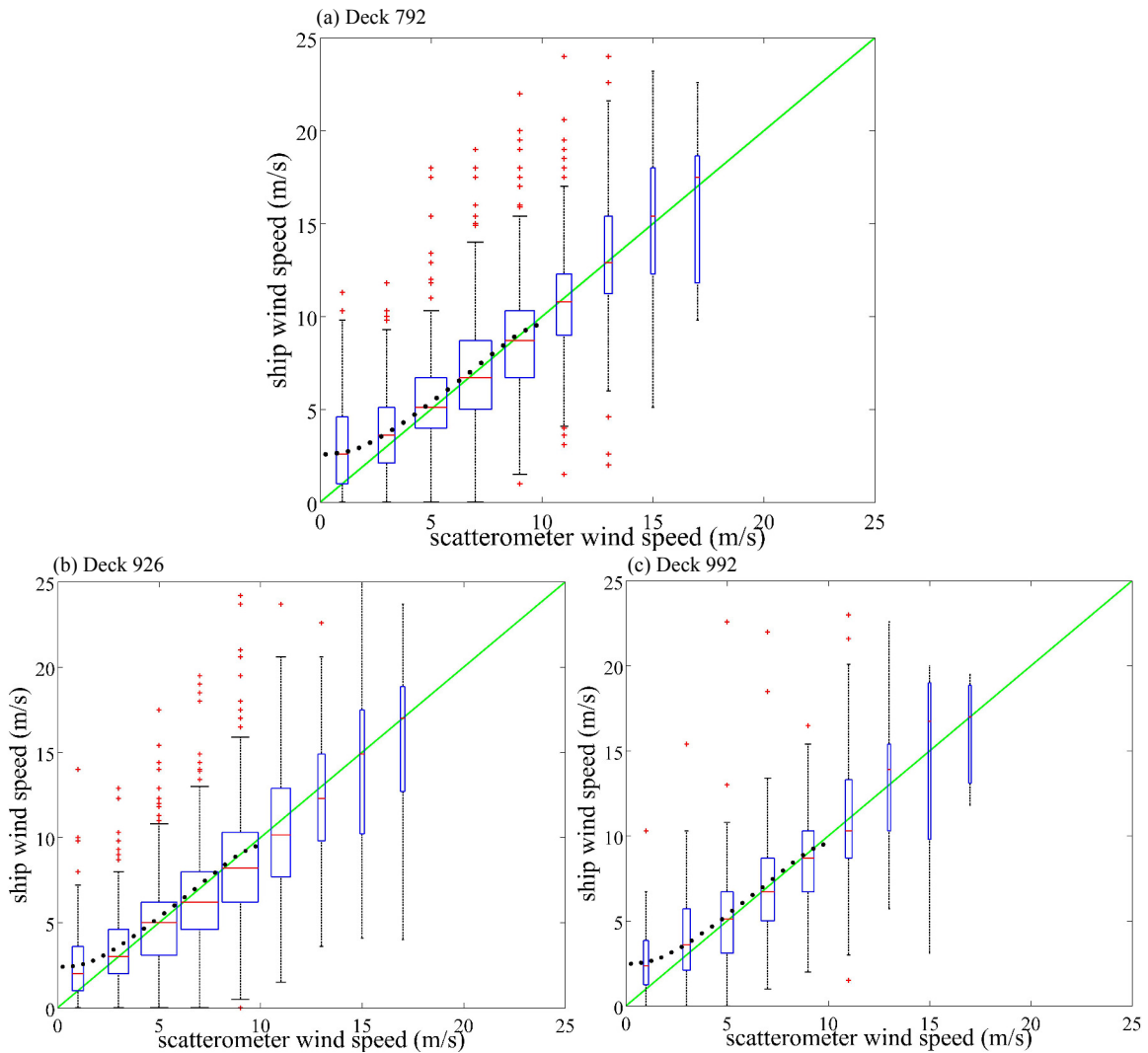


Figure 10. Same as Figure 9. The black dots are associated with conditional sample mean of simulated noisy dataset within each 0.5ms^{-1} bin of the simulated error-free dataset. (a) Deck 792; (b) Deck 926; (c) Deck 992.

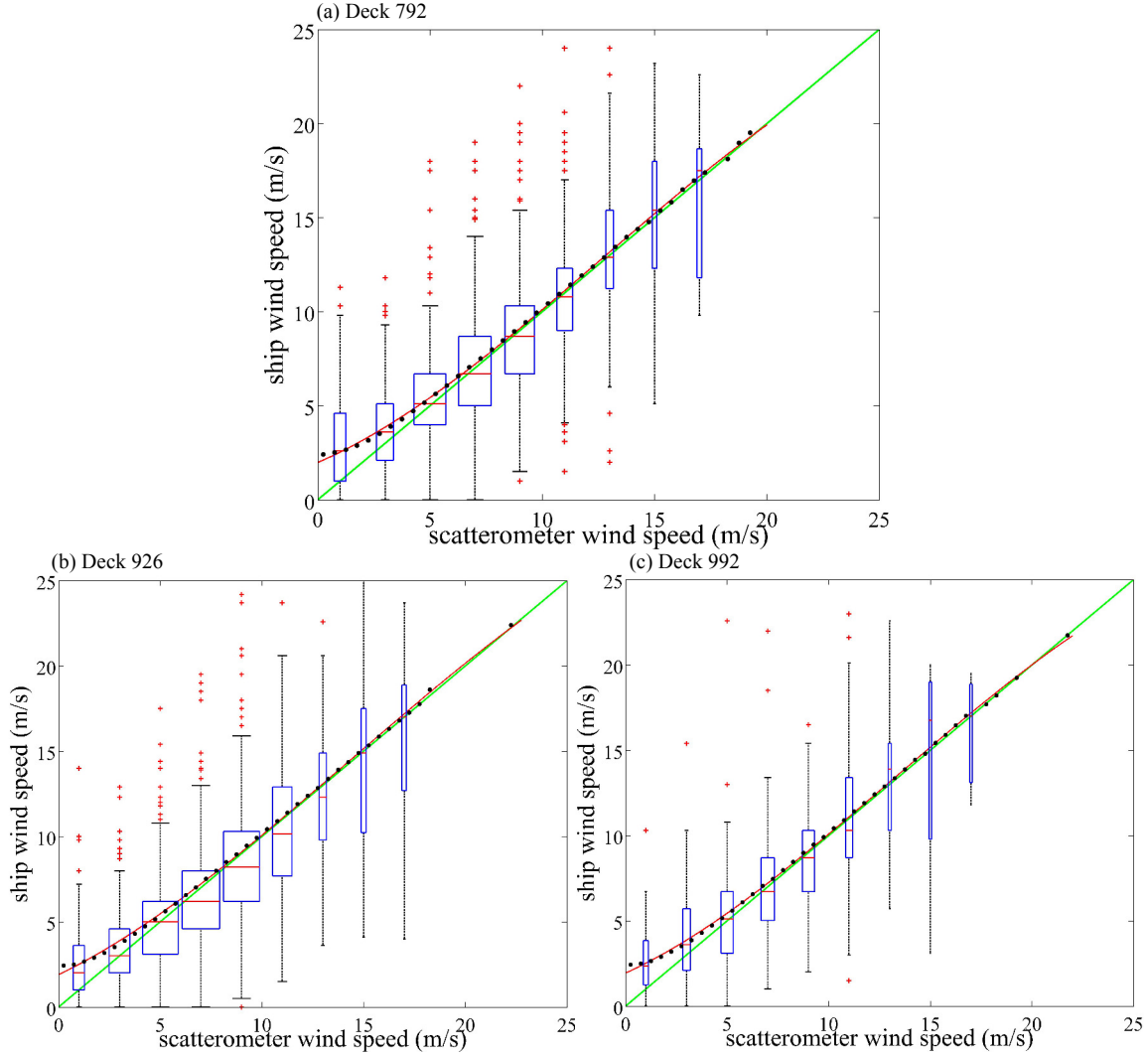


Figure 11: Same as Figure 9. The black dots are associated with conditional sample mean of each 0.5ms^{-1} bin of scatterometer winds generated by Monte Carlo approach. Red line is the cubic fitting line for those black dots (conditional sample mean). (a) Deck 792; (b) Deck 926; (c) Deck 992.

A statistical significance test is conducted for each bin in order to account for statistical artifacts associated with the large random errors in the collocated estimated ship winds. In the present study, two-tailed t-test is used and $\alpha=0.01$. We did not use z-test because the exact standard deviation of the estimated ship winds is not known.

Table 2 details, for each bin, whether or not it is necessary to apply the bias correction by removing the artificial bias in the ship winds. ‘N/A’ means empty; this is because of the temporal and spatial mismatches within that range of wind speed in collocation. Where P-value is less than α ($\alpha = 0.01$), it is necessary to apply the bias correction. The result of statistical significance testing rounding to three decimal place with deck 792 and deck 992 reveals that most of bins of

wind speed from these two decks are identified as artifact random error, meaning the bias correction does not need to be applied, and that visually-estimated winds are very well calibrated to satellite winds, albeit much noisier than satellite winds. This result is consistent with the results from the previous analysis that revealed the wind speed in decks 792 and 992 show a close match between the conditional sample mean and the medians of boxplot.

Table 2. Statistical significance test for deck 792 and deck 992. Those P-values less than α are bolded.

Wind speed range (ms ⁻¹)	P-value		Wind speed range (ms ⁻¹)	P-value	
	Deck 792	Deck 992		Deck 792	Deck 992
0.0-0.5	0.210	0.049	10.0-10.5	0.595	0.026
0.5-1.0	0.993	0.896	10.5-11.0	0.112	0.136
1.0-1.5	0.843	0.430	11.0-11.5	0.032	0.646
1.5-2.0	0.268	0.070	11.5-12.0	0.451	0.667
2.0-2.5	0.042	0.622	12.0-12.5	0.893	0.884
2.5-3.0	<0.001	<0.001	12.5-13.0	0.764	0.275
3.0-3.5	0.923	0.235	13.0-13.5	0.230	0.100
3.5-4.0	0.321	<0.001	13.5-14.0	0.451	0.919
4.0-4.5	0.592	0.674	14.0-14.5	0.583	0.702
4.5-5.0	0.356	0.002	14.5-15.0	0.759	0.058
5.0-5.5	0.019	0.007	15.0-15.5	0.389	0.059
5.5-6.0	0.661	<0.001	15.5-16.0	0.197	0.152
6.0-6.5	0.614	<0.001	16.0-16.5	0.235	0.203
6.5-7.0	0.110	0.069	16.5-17.0	0.511	0.024
7.0-7.5	0.002	0.028	17.0-17.5	0.935	N/A
7.5-8.0	0.261	0.002	17.5-18.0	N/A	0.953
8.0-8.5	0.160	0.039	18.0-18.5	0.640	0.895
8.5-9.0	0.005	0.594	18.5-19.0	0.261	N/A
9.0-9.5	0.012	<0.001			
9.5-10.0	0.527	0.021			

In order to address the bias for each bin of wind speed, we use the following formula:

$$bias = w_{ship} - error_{artifact} - w_{scat} \quad (4.1)$$

Where w_{ship} denotes the median of ship winds in each bin of satellite winds due to the larger effect of outlier on mean rather than median; $error_{artifact}$ denotes the artifact difference; and w_{scat} denotes the mean for each bin of satellite winds. By removing the artifact error from the collocated ship winds, the correction for real biases can be addressed by the difference between collocated ship winds with artifact biases removed and satellite winds within each 0.5ms⁻¹ bin. This method of addressing bias correction is applied to decks 792 and 992, thus two sets of bias correction values are calculated, as shown in Table 3. Applying these two bias corrections for the

corresponding decks (792 and 992) is a straightforward process. The bias correction value is applied to the wind speed range, which can be confidently identified as a bias based on the statistical significance test.

For other wind speeds, a new bias correction can be calculated through a weighted average of those two bias correction values by the number of observations for deck 792 and deck 992. This new bias correction is limited up to 17ms^{-1} . This is because, both for deck 792 and deck 992, no collocated matches are found within a 0.5ms^{-1} bin of wind speeds ranging from 17ms^{-1} to 19ms^{-1} . We use a cubic interpolator to calculate the corresponding bias correction value for each specific wind speed value. This new bias correction is referred to as the ‘LMS’ correction.

Table 3. Bias correction for decks 792 and 992.

Wind speed range (ms^{-1})	Bias correction		Wind speed range (ms^{-1})	Bias correction	
	Deck 792	Deck 992		Deck 792	Deck 992
0.0-0.5	-1.521	-1.415	10.0-10.5	-0.157	-0.630
0.5-1.0	-0.003	0.083	10.5-11.0	-0.652	-0.609
1.0-1.5	-0.157	-0.594	11.0-11.5	0.856	0.145
1.5-2.0	-0.368	-0.558	11.5-12.0	0.374	0.241
2.0-2.5	-0.632	-0.127	12.0-12.5	-0.099	-0.108
2.5-3.0	1.004	0.484	12.5-13.0	0.257	0.533
3.0-3.5	0.049	-0.283	13.0-13.5	1.538	0.004
3.5-4.0	0.253	-1.194	13.5-14.0	-0.990	0.135
4.0-4.5	0.240	-0.131	14.0-14.5	-0.517	-0.493
4.5-5.0	-0.202	-0.555	14.5-15.0	0.419	1.167
5.0-5.5	-0.567	-0.501	15.0-15.5	2.119	3.067
5.5-6.0	-0.115	-0.998	15.5-16.0	3.173	-2.455
6.0-6.5	0.107	-1.464	16.0-16.5	-2.594	-1.001
6.5-7.0	-0.373	-0.352	16.5-17.0	-1.581	2.027
7.0-7.5	-0.833	-0.476	17.0-17.5	0.113	N/A
7.5-8.0	-0.303	-0.773	17.5-18.0	N/A	0.292
8.0-8.5	-0.488	-0.459	18.0-18.5	-0.158	-0.250
8.5-9.0	-0.777	-0.138	18.5-19.0	-8.632	N/A
9.0-9.5	-0.759	-1.275			
9.5-10.0	-0.160	-0.613			

This new LMS bias correction is compared to Lindau’s (1995) correction. Table 4 illustrates that at Beaufort force 1, which is associated with wind speeds of 0ms^{-1} , Lindau (1995) suggests a bias correction of 0.0ms^{-1} whereas the LMS correction suggests -0.2ms^{-1} as the bias correction value. This value is consistent with the global average bias of 0.2ms^{-1} between equivalent neutral winds (larger; referring to satellite scatterometer winds) and actual winds

(referring to estimated ship winds). At Beaufort forces 1 and 4, the Lindau (1995) and LMS corrections have the same adjusted value (0.2ms^{-1} and 0.5ms^{-1} respectively). The LMS correction at Beaufort forces 2 and 3 is much greater than Lindau's (1995) correction, and at a Beaufort force 5, the LMS correction is less than Lindau's (1995) correction. Both the LMS and Lindau (1995) corrections indicate a negative bias correction value, although not identical. However, this new bias correction is only available for the wind speed range 0ms^{-1} - 17ms^{-1} , which is limited to spatial and temporal matches in the collocation process.

Table 4. The comparison between Lindau's (1995) correction and LMS correction

Beaufort Force	Wind speed value in WMO 1100 scale (ms^{-1})	Lindau's (1995) correction value (ms^{-1})	LMS correction value (ms^{-1})
0	0.0	0.0	0.2
1	1.0	-0.2	-0.2
2	2.6	-0.1	-0.5
3	4.6	-0.0	-0.6
4	6.7	-0.5	-0.5
5	9.3	-0.4	-0.1
6	12.3	0.2	0.3
7	15.4	0.8	0.3
8	19.0	1.8	--
9	22.6	2.4	--
10	26.8	3.4	--
11	30.9	3.8	--
12	--	--	--

CHAPTER 5

CONCLUSION

The purpose of this study was to improve the conversion of the Beaufort estimates scale to geophysical numeric wind speeds with scientific units (ms^{-1} in this case). While the initial plan was to use the Lindau's (1995) correction, in analyzing the visually estimated ship winds in ICOADS it was found to be unsuitable. Thus ultimately, an entirely new bias correction was developed using intercalibration between satellite scatterometer winds and visually estimated ship winds.

The author concluded that use of the Lindau (1995) correction would not be applicable when an initial analysis of the visually estimated ship winds in the ICOADS showed that most of the estimated ship winds for each major deck did not have the anticipated '13 value' wind speed distribution. This is because observation practices vary by country and data provider (different deck numbers indicate different data collections provided to ICOADS, each which may contain one or more sources/countries). Because the wind speed indicator (WI)=5 is known to be Beaufort winds (converted based on WMO 1100 scale), it was not surprising that the deck 761 dataset with WI=5 fell into the 13 discrete bins consistent with the Beaufort scale classifications (0 to 12). However, the distribution of wind speeds with WI= 0, 2 (not shown in this study), 3 or 6 for other major ICOADS decks revealed many more than the anticipated 13 bins.

Therefore, assuming that the visually estimated ship winds and scatterometer winds have similar adjustments to 10m equivalent neutral winds, we calculated a new bias correction (referred to as the LMS correction) through a comparison between the QuickSCAT scatterometer winds and collocated visually estimated ship winds in ICOADS. This new calibration results in a revised bias correction for historical calibrations.

It is notable that Lindau (1995) did extraordinary work through a rigorous derivation by considering the equal error variance in a two-way regression, but the Lindau (1995) scale relied on pressure gradients for comparison data, where these gradients had considerable uncertainty. This approach uses better comparison data, and applies more detailed analyses for very low and very high wind speeds. By applying the Freilich (1997) model to test the statistical artificial biases in the component of vector wind speeds at high/low boundaries, the author concluded that

the artificial biases have a significant effect on the lower wind speeds (0ms^{-1} to 5ms^{-1}) and little impact on the higher wind speeds (14ms^{-1} to 20ms^{-1}). These artificial biases are properly accounted for in the new LMS calibration, which is limited up to 17ms^{-1} of wind speed. Because of the intercalibration between satellite winds and collocated ship winds that met severe quality control requirements, very few temporal and spatial matches were found in the higher wind speed areas. Future work will investigate ways to further improve this bias correction and calculate the bias correction for wind speed greater than 17ms^{-1} . In the meantime, the LMS-adjusted estimated ship wind speed data will be provided in the *ivad attm* embedded into the next advanced version of ICOADS (ICOADS R3.0).

The results of this study will have additional benefits in a variety of ways. For example, this study serves to validate satellite data, which is an important step in the development of new products and retrieval algorithms by the remote sensing community and satellite data assimilation groups. IVAD project aims to provide ‘best’ adjustment for marine observations (e.g. visually estimated ship winds), and by collaborating with the reanalysis community (e.g., the ERA-Interim Climatology and 20th Century Reanalysis Group), ICOADS will be made aware of systematic errors, thereby allowing for additional improvements to the bias adjustment for marine observations (e.g. estimated ship winds).

Finally, by making ICOADS more homogenous through the application of bias adjustments (e.g., Beaufort wind adjustments), it will be more useful to the wider scientific community. And the assurance of a more formal (and uniform) international repository, ICOADS/IVAD will encourage closer linkages between international research communities.

REFERENCES

- Berry, D.I., E. C. Kent, and P. K. Taylor, 2004: An analytical model of heating errors in marine air temperatures from ships. *J. Tech.*, **21**(8), 1198-1215, doi:[http://dx.doi.org/10.1175/1520-0426\(2004\)021<1198:AAMOHE>2.0.CO;2](http://dx.doi.org/10.1175/1520-0426(2004)021<1198:AAMOHE>2.0.CO;2)
- Boukabara, S.A., R.N.Hoffman, and C.Grassotti, 2000: Atmospheric Compensation and Heavy Rain Detection for SeaWinds Using AMSR, *Atmos. Environ. Res. Inc.*, 131 Hartwell Ave., Lexington, Massachusetts (USA), 2000.
- Bourassa, M. A., D. M. Legler, J. J. O'Brien, and S. R. Smith, 2003: SeaWinds validation with research vessels. *J. Geophys. Res.*, **108**, 3019, doi:10.1029/2001JC001028.
- Bourassa, M. A., 1998: Equivalent Neutral winds. Center of Ocean-Atmospheric Prediction Studies (COAPS) at Florida State University (FSU). Accessed 17 July 1998. [Available online at https://coaps.fsu.edu/~bourassa/BVW_html/eqv_neut_winds.shtml.]
- Bourassa, M. A., R. Romero, S. R. Smith, and J. J. O'Brien, 2005: A New FSU Winds Climatology. *J. Climate*, **18**, 3686–3698, doi: <http://dx.doi.org/10.1175/JCLI3487.1>
- Cardone, V. J., 1969: Specification of the wind distribution in the marine boundary layer for wave forecasting. Rep. TR69-1, Dept. of Meteorology and Oceanography Geophysical Sciences, Laboratory, New York University School of Engineering and Science, New York, NY, 131 pp. [NTIS AD 702 490.]
- daSilva, A. M., C. C. Young, and S. Levitus, 1994: *Atlas of Surface Marine Data 1994*. Vol. 2, *Anomalies of Directly Observed Quantities*, NOAA, 416 pp.
- Dupigny-Giroux, LA, T. F. Ross, J. D.Elms, R.Truesdell, S. R. Doty, 2007: NOAA's Climate Database Modernization Program: Rescuing, Archiving, and Digitizing History. *Bull. Amer. Meteor. Soc.*, **88**, 1015–1017.
- Draper, D. W. and D. G. Long, 2004: Simultaneous wind and rain retrieval using SeaWinds data. *IEEE Trans. Geosci. Remote Sens.*, **42**, 1411–1423, doi: 10.1109/TGRS.2004.830169
- Fore, A. G., B. W. Stiles, A. H. Chau, B. A. Williams, R. S. Dunbar, and E. Rodríguez, 2014: Point-Wise wind retrieval and ambiguity removal improvements for the QuikSCAT climatological data set. *IEEE Trans. Geosci. Electron.*, **52**, 51-59, doi: 10.1109/TGRS.2012.2235843
- Freilich, M. H., 1997: Validation of Vector Magnitude Datasets: Effects of Random Component Errors. *J. Atmos. Oceanic Technol.*, **14**, 695–703, doi: [http://dx.doi.org/10.1175/1520-0426\(1997\)014<0695:VOVMDE>2.0.CO;2](http://dx.doi.org/10.1175/1520-0426(1997)014<0695:VOVMDE>2.0.CO;2)
- Freilich, M. H., and R. S. Dunbar, 1999: The accuracy of the NSCAT 1 vector winds: Comparisons with National Data Buoy Center buoys, *J. Geophys. Res.*, **104**, 11231–11246,

doi: 10.1029/1998JC90009

Hoffman, R. N., C. Grassotti, and S. M. Leidner, 2004: Seawinds validation: Effect of rain as observed by East Coast radars. *J. Atmos. Oceanic Technol.*, **21**, 1364–1377, doi: [http://dx.doi.org/10.1175/1520-0426\(2004\)021<1364:SVEORA>2.0.CO;2](http://dx.doi.org/10.1175/1520-0426(2004)021<1364:SVEORA>2.0.CO;2)

Huddleston, J.N., and B.W. Stiles, 2000: A Multi-dimensional Histogram Technique for Flagging Rain Contamination on QuikSCAT, *Proc. IEEE Int. Geoscience and Remote Sensing Symp. 2000*, Honolulu, HI, **3**, 1232-1234, doi:10.1109/IGARSS.2000.858077

Isemer, H.-J., 1992: Comparison of estimated and measured marine surface winds. *Proc. Int. COADS Workshop*, Boulder, CO, NOAA/ERL, 143–158.

JPL, 1999: QuikSCAT science data product user's manual. Version 1.1, Jet Propulsion Laboratory D-18053, 84 pp.

JPL, 2013: QuikSCAT Level 2B Ocean Wind Vectors in 12.5km Slice Composites Version 3. Accessed 1 March 2016. [Available online at https://podaac.jpl.nasa.gov/dataset/QSCAT_LEVEL_2B_OWV_COMP_12], doi: 10.5067/QSX12-L2B01

Kara, A. B., A. J. Wallcraft, and M. A. Bourassa, 2008: Air-sea stability effects on the 10 m winds over the global ocean: evaluations of air-sea flux algorithms. *J. Geophys. Res.*, **113**: C04009, doi: 10.1029/2007JC004324

Kaufeld, L., 1981: The development of a new Beaufort equivalent scale. *Meteor. Rundsch.*, **34**, 17–23.

Kent, E. C. and P. K. Taylor, 1997: Choice of a Beaufort Equivalent Scale. *J. Atmos. Oceanic Technol.*, **14**, 228–242, doi: [http://dx.doi.org/10.1175/1520-0426\(1997\)014<0228:COABES>2.0.CO;2](http://dx.doi.org/10.1175/1520-0426(1997)014<0228:COABES>2.0.CO;2)

Lindau, R., 1995: A new Beaufort equivalent scale. *Proc. Int. COADS Winds Workshop*, Kiel, Germany, Institut für Meereskunde Kiel and NOAA, 232–252.

Mears, C. A., D. K. Smith, and F. J. Wentz, 2001: Comparison of Special Sensor Microwave Imager and buoy-measured wind speeds from 1987 to 1997, *J. Geophys. Res.*, **106**, 11,719–11,729, doi: 10.1029/1999JC000097

National Climatic Data Center/NESDIS/NOAA/U.S. Department of Commerce, Data Support Section/Computational and Information Systems Laboratory/National Center for Atmospheric Research/University Corporation for Atmospheric Research, Earth System Research Laboratory/NOAA/U.S. Department of Commerce, and Cooperative Institute for Research in Environmental Sciences/University of Colorado. 1984, updated monthly. *International Comprehensive Ocean-Atmosphere Data Set (ICOADS) Release 2.5, Individual Observations*. Research Data Archive at the National Center for Atmospheric Research, Computational and

Information Systems Laboratory. <http://dx.doi.org/10.5065/D6H70CSV>. Accessed 25/06/2012.

Portabella, M., and Stoffelen, A., 2001: Rain Detection and Quality Control of Sea Winds, *J. Atmos. Oceanic Technol.*, **18**, 1171-1183, doi: [http://dx.doi.org/10.1175/1520-0426\(2001\)018<1171:RDAQCO>2.0.CO;2](http://dx.doi.org/10.1175/1520-0426(2001)018<1171:RDAQCO>2.0.CO;2).

Ramage, C. S., 1987: Secular Changes in Reported Surface Wind Speeds Over the Ocean. *J. Appl. Meteorol.* **26**, 525–528, doi: [10.1175/1520-0450\(1987\)026<0525:SCIRSW>2.0.CO;2](https://doi.org/10.1175/1520-0450(1987)026<0525:SCIRSW>2.0.CO;2).

Ross, D. B., V. J. Cardone, J. Overland, R. D. McPherson, W. J. Pierson Jr., T. Yu, 1985: Oceanic surface winds. *Adv. Geophys.*, **27**, 101–138.

Slutz, R. J., S. J. Lubker, J. D. Hiscox, S. D. Woodruff, R. L. Jenne, D. H. Joseph, P. M. Steurer, and J. D. Elms, 1985: Comprehensive Ocean-atmosphere Data Set; Release 1. NOAA Environmental Research Laboratories, Climate Research Program: Boulder, CO; 268, (NTIS PB86-105723). URL: http://icoads.noaa.gov/Release_1/coads.html

Sobieski, P. W., C. Craeye, and L. F. Bliven, 1999: Scatterometric signatures of multivariate drop impacts on fresh and salt water surfaces. *Int. J. Remote Sens.*, **20**, 2149–2166, doi: [10.1080/014311699212164](https://doi.org/10.1080/014311699212164).

Tang, W., and W. T. Liu, 1996: Equivalent Neutral Wind, JPL Publication 96-17.

Verschell, M. A., M. A. Bourassa, D. E. Weissman, and J. J. O'Brien, 1999: Model Validation of the NASA Scatterometer Winds. *J. Geophys. Res.*, **104**, 11,359-11,374, doi: [10.1029/1998JC900105](https://doi.org/10.1029/1998JC900105).

Thomas, B. R., E. C. Kent, V. R. Swail, and D. I. Berry, 2008: Analysis of Monthly Mean Marine Winds Adjusted for Observation Method and Height. *Int. J. Climatol.*, **28**, 747–763, doi: [10.1002/joc.1570](https://doi.org/10.1002/joc.1570).

Weissman, D., M. A. Bourassa, and J. Tongue, 2002: Effects of rain rate and magnitude on SeaWind scatterometer wind speed errors. *J. Atmos. Oceanic Technol.*, **19**, 738–746.

Weissman, D.E. and M.A. Bourassa, 2008: Measurements of the effect of rain-induced sea surface roughness on the satellite scatterometer radar cross section. *IEEE Trans. Geosci. Remote Sens.*, **46**, 2,882–2,894, doi: [10.1109/TGRS.2008.2001032](https://doi.org/10.1109/TGRS.2008.2001032).

Weissman, D.E. and 6 others (2012), Challenges to Satellite Sensors of Ocean Winds: Addressing Precipitation Effects. *J. Atmos. Oceanic Technol.*, **29**(3), 356–374, doi: [10.1175/JTECH-D-11-00054.1](https://doi.org/10.1175/JTECH-D-11-00054.1).

WMO, 1970: The Beaufort scale of wind force (Technical and operational aspects). Commission for Marine Meteorology, Rep. on Marine Science Affairs 3, 22 pp. [Available from World Meteorological Organization, Case Postale 5, Geneva, Switzerland.]

WMO, 1980: International list of selected, supplementary, and auxiliary ships, WMO 47.

[Available from World Meteorological Organization, Case Postale 5, Geneva, Switzerland.]

Woodruff, S. D., and Coauthors, 2011: ICOADS Release 2.5: Extensions and Enhancements to the Surface Marine Meteorological Archive. *Int. J. Climatol.*, **31**, 951-967, doi: 10.1002/joc.2103

Woodruff, S. D., and Coauthors, 2015: Proposed IMMA revisions (*Revised DRAFT, 19 August 2015 (v21)*), R3.0-imma_short. Available online at <http://icoads.noaa.gov/ivad/IMMA-Rev.pdf>

Wright, P. B, 1988: On the Reality of Climatic Changes in Wind Over the Pacific. *Int. J. Climatol.*, **8**, 521–527, doi: 10.1002/joc.3370080508

SeaPAC, 2013: QuikSCAT Level 2B Ocean Wind Vectors in 12.5km Slice Composites Version 3. Ver. 3. PO.DAAC, CA, USA. Dataset accessed [2012-01-01] at <http://dx.doi.org/10.5067/QSX12-L2B01>.

BIOGRAPHICAL SKETCH

Keqiao Li was raised in Chifeng city, Inner Mongolia, China. After receiving a B.S. in Marine Science (Remote Sensing and Data Processing), he became a Seminole and major in Atmospheric Science and Meteorology at Florida State University. During his master study under the supervision of Dr. Mark A. Bourassa, his passion in Remote Sensing and statistical application in Meteorology was strengthened. Upon completing his master's degree, Keqiao intends to pursue a Ph.D. in Meteorology. Beyond his academic interests, he also enjoys playing badminton and accordion, which make his life more colorful.